

Detection Technique to Mitigate Kerr Effect Phase Noise

Keang-Po Ho and Joseph M. Kahn

Abstract—Kerr effect phase noise, often called the Gordon-Mollenauer effect, can be compensated by subtracting from the received phase a correction proportional to the received intensity. In this paper, we describe how to perform this compensation in the electrical domain, and analytically determine the optimal scale factor for the correction. Using optimal compensation, the standard deviation of residual phase noise is halved, doubling the transmission distance in systems limited by Kerr effect phase noise.

Index Terms—Phase Detection, Fiber Nonlinearities, Phase Noise

I. INTRODUCTION

GORDON and Mollenauer [1] showed that when optical amplifiers are used to compensate for fiber loss, the interaction of amplifier noise and the Kerr effect causes phase noise, even in systems using constant-intensity modulation. This Kerr effect phase noise, also called the Gordon-Mollenauer effect, corrupts the received phase and limits transmission distance in systems using phase-shift keying (PSK) or differential phase-shift keying (DPSK). These classes of constant-intensity modulation techniques have received renewed attention recently for long-haul and/or spectrally efficient WDM applications [2]-[4]. Recently, the received intensity is used to compensate the Kerr effect phase noise [5]-[6]. Previous compensation methods have used a nonlinear optical component [5] or a phase modulator [6]. In this letter, we describe how to perform the compensation using electronic circuits. We derive the optimal correction factor for this electronic compensation, which can also be applied to optimize the methods of [5]-[6]. The optimal compensation can halve the standard deviation (STD) of Kerr effect phase noise, doubling the transmission distance in systems whose dominant impairment is Kerr effect phase noise.

II. CORRECTION OF KERR EFFECT PHASE NOISE

We consider a system with many fiber spans using an optical amplifier in each span to compensate for fiber loss. For simplicity, we assume that each span is of the same length, and

that an identical optical power is launched into each span. In the linear propagation regime, the electric field launched in the k th span is equal to $E_k = E_0 + n_1 + n_2 + \dots + n_k$, $k = 1 \dots N$, where E_0 is the transmitted signal, and n_k , $k = 1 \dots N$, is the complex amplifier noise at the k th span. For a system using binary phase shift-keying (BPSK), $E_0 \in \pm A$. The variance of n_k is $E\{|n_k|^2\} = 2\sigma^2$, $k = 1 \dots N$, where σ^2 is the noise variance per span per dimension. In the linear regime, ignoring the fiber loss of the last span and the amplifier gain required to compensate it, the signal received after N spans is $E_N = E_0 + n_1 + n_2 + \dots + n_N$.

Kerr effect phase noise is accumulated span by span, and the overall nonlinear phase shift is equal to [1]

$$\phi_{NL} = \gamma L_{\text{eff}} \left\{ |E_0 + n_1|^2 + |E_0 + n_1 + n_2|^2 + \dots + |E_0 + n_1 + \dots + n_N|^2 \right\} \quad (1)$$

where γ is the nonlinear coefficient of the fiber, and L_{eff} is the effective nonlinear length per fiber span. In the presence of Kerr effect phase noise, the received electric field is $E_R = E_N \exp(-j\phi_{NL})$. In PSK systems, an optical phase-locked loop (PLL) [7] can be used to receive the in-phase and quadrature components of the received electrical field E_R . In DPSK systems, a pair of interferometers [3] can be used to obtain both in-phase and quadrature differential components of the received electrical field E_R .

Fig. 1 shows the simulated distribution of the received electric field E_R , detected by an optical PLL (e.g., see Fig. 5 of [7]), in a BPSK system with $N = 32$ spans. The received optical signal-to-noise ratio (OSNR) is $A^2/(2N\sigma^2) = 18$, corresponding to a bit-error rate (BER) of 10^{-9} in the linear regime. In Fig. 1a, the mean nonlinear phase is $\langle \phi_{NL} \rangle = 1$ rad, corresponding to the maximum mean nonlinear phase shift estimated in [1]. Fig. 1b illustrates the case $\langle \phi_{NL} \rangle = 2$ rad. The helical-shaped distributions in Figs. 1 arise because the nonlinear phase rotation is correlated with the received intensity [5]-[6]. Figs. 1 also show spiral curves that separate the plane into two decision regions. These decision regions resemble the Yin-Yang logo of Chinese mysticism, and are called the “Yin-Yang detector” below. The Yin-Yang detector uses strictly electronic techniques to compensate Kerr effect phase noise, and hence, it differs significantly from the optical [5] and electro-optical [6] compensation techniques considered previously.

In an N -span system, to first order, the optimal correction

Manuscript received October 3, 2002, revised November 22, 2002.

K.-P. Ho is with StrataLight Communications, Campbell, CA 95008, USA. (Tel: 408-961-6259, Fax: 408-626-7100, e-mail: kpho@stratalight.com)

J. M. Kahn is with StrataLight Communications, Campbell, CA 95008, and Department of Electrical Engineering and Computer Sciences, University of California, Berkeley, CA 94720. (e-mail: jmk@eecs.berkeley.edu)

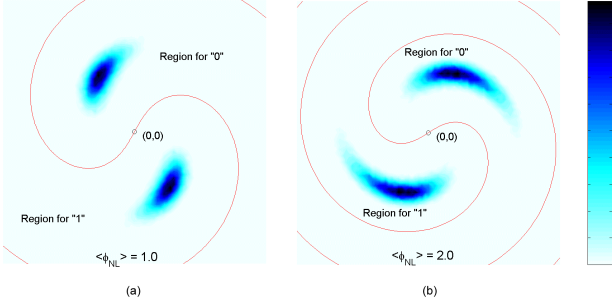


Fig. 1. Simulated distribution and decision regions of received signal with Kerr effect phase noise for various mean nonlinear phase shifts: (a) $\langle \phi_{NL} \rangle = 1$ rad and (b) $\langle \phi_{NL} \rangle = 2$ rad.

term can be derived by finding a scale factor α to minimize the variance of the residual nonlinear phase shift $\phi_{NL} + \alpha P_N$. The corrected phase estimate is $\phi_R - \alpha P_N$, where ϕ_R is the phase of the received electric field E_R . After some algebra, as shown in the Appendix, the optimal scale factor is found to be

$$\alpha = -\gamma L_{\text{eff}} \frac{N+1}{2} \cdot \frac{|E_0|^2 + (2N+1)\sigma^2/3}{|E_0|^2 + N\sigma^2} \approx -\gamma L_{\text{eff}} \frac{N+1}{2}. \quad (2)$$

The variance of the residual nonlinear phase shift is reduced to

$$\begin{aligned} \sigma_{\phi_{NL} + \alpha P_N}^2 &= (N-1)N(N+1)(\gamma L_{\text{eff}} \sigma)^2 \\ &\quad \times \frac{|E_0|^4 + 2N\sigma^2 |E_0|^2 + (2N^2+1)\sigma^4/3}{3(|E_0|^2 + N\sigma^2)} \\ &\approx \frac{N^3(\gamma L_{\text{eff}} \sigma |E_0|)^2}{3} \approx \frac{\langle \phi_{NL} \rangle^2}{6\text{OSNR}} \end{aligned} \quad (3)$$

from

$$\begin{aligned} \sigma_{\phi_{NL}}^2 &= \frac{2}{3}N(N+1)(\gamma L_{\text{eff}} \sigma)^2 [(2N+1)|E_0|^2 + (N^2+N+1)\sigma^2] \\ &\approx \frac{4N^3(\gamma L_{\text{eff}} \sigma |E_0|)^2}{3} \approx \frac{2\langle \phi_{NL} \rangle^2}{3\text{OSNR}}. \end{aligned} \quad (4)$$

In (2) to (4), the approximate equalities are valid for high OSNR and for large N , which is the situation of practical interest. The mean nonlinear phase shift is

$$\langle \phi_{NL} \rangle = N\gamma L_{\text{eff}} [|E_0|^2 + (N+1)\sigma^2] \approx N\gamma L_{\text{eff}} |E_0|^2. \quad (5)$$

To our knowledge, the optimal scale factor (2) and variance of residual phase noise (3) have been derived here for the first time. While [8] considered a more complicated system, the simple approximation in (4) may yield more useful insight. We should note that in [6], simulation was used to optimize the scale factor, yielding a result similar to (2).

Figs. 2 show the distribution of the corrected signal $E_c = E_R \exp(-j\alpha P_N)$, assuming the same parameters as Figs. 1. The distributions shown in Figs. 2 have been rotated by the mean phase $\langle \phi_{NL} + \alpha P_N \rangle$, so that the decision regions become the right and left half-planes. Comparing Figs. 1 to Figs. 2, we see that the phase correction has dramatically reduced the STD of the nonlinear phase shift. Note that, ignoring a rotation, the phase distribution in Fig. 2b is similar to that in Fig. 1a.

Decoding the corrected electric field E_c using the right and left half-planes in Figs. 2 is equivalent to decoding the

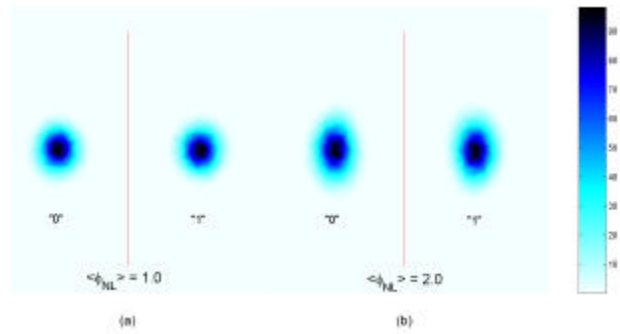


Fig. 2. Simulated distribution of corrected signal using optimal correction factor for various mean nonlinear phase shifts: (a) $\langle \phi_{NL} \rangle = 1$ rad and (b) $\langle \phi_{NL} \rangle = 2$ rad.

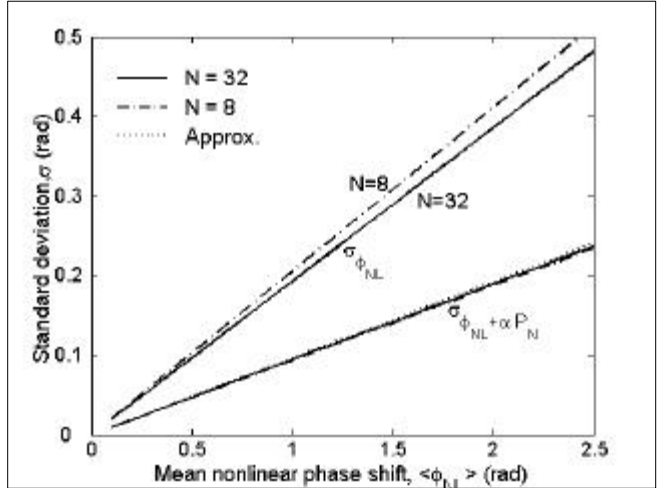


Fig. 3. The standard deviation of Kerr effect phase noise as a function of the absolute mean nonlinear phase noise $|\langle \phi_{NL} \rangle|$ for $N = 8$ and 32 spans.

received electric field E_R using the Yin-Yang decision regions shown in Figs. 1. These spiral curves are rotated versions of $\phi - \alpha \rho^2 = 0$, where ρ and ϕ are the radius and phase in polar coordinates.

Fig. 3 shows the STDs $\sigma_{\phi_{NL}}$ and $\sigma_{\phi_{NL} + \alpha P_N}$, given by (4) and (3), as functions of the mean nonlinear phase shift $\langle \phi_{NL} \rangle$ of (5), for $N = 8$ and 32 spans. Fig. 3 assumes OSNR = 18, like Figs. 1 and 2. Fig. 3 also indicates the approximations

$\sigma_{f_{NL}} \approx 0.1925 \langle f_{NL} \rangle$ and $\sigma_{\phi_{NL} + \alpha P_N} \approx 0.0962 \langle \phi_{NL} \rangle$, (6) obtained from (4) and (3), as dotted lines. When the correction factor (2) is employed, the STD of the residual nonlinear phase shift $\sigma_{\phi_{NL} + \alpha P_N}$ is nearly independent of the number of fiber spans, and is very close to the approximation in (6). For a given value of the mean nonlinear phase shift $\langle \phi_{NL} \rangle$, the STD of the nonlinear phase shift $\sigma_{\phi_{NL}}$ decreases with increasing N . For $N = 32$, $\sigma_{\phi_{NL}}$ is indistinguishable from the approximation given by (6). Fig. 3 demonstrates that for large N , our phase correction scheme reduces the STD of Kerr effect phase noise by a factor of two.

III. DISCUSSION

Gordon and Mollenauer [1] estimated that the Kerr effect

phase noise-limited transmission distance is limited to a value such that the mean nonlinear phase shift is $\langle \phi_{NL} \rangle = 1$ rad. From Fig. 3 and (6), this corresponds to a STD of $\sigma_{\phi_{NL}} \approx 0.1925$ rad. Because a mean phase conveys neither information nor noise, while the STD of phase $\sigma_{\phi_{NL}}$ is an indicator of system impairment, we can restate the condition for maximum transmission distance in terms of STD of phase as $\sigma_{\phi_{NL}} \approx 0.1925$ rad. Using our phase correction scheme (or the Yin-Yang detector) and allowing the STD of corrected phase to take on the same value, i.e., $\sigma_{\phi_{NL} + \alpha P_N} = 0.1925$ rad, corresponds to a mean nonlinear phase shift of $\langle \phi_{NL} \rangle = 2$ rad. Because the mean nonlinear phase shift is proportional to the number of fiber spans as shown in (5), doubling the mean nonlinear phase shift doubles the number of fiber spans, and thus doubles the transmission distance, assuming that the Kerr effect phase noise is the primary limitation.

While the foregoing discussion has focused on BPSK, the use of DPSK has generated much more interest recently [2-7]. In a DPSK system, information is encoded in phase differences between successive symbols, and is decoded using the differential phase $\phi_R(t+T) - \phi_R(t)$, where T is the symbol interval. When the differential phase is corrupted by the nonlinear phase shift difference $\phi_{NL}(t+T) - \phi_{NL}(t)$, the impact of Kerr effect phase noise can be compensated by decoding $\phi_R(t+T) - \phi_R(t) - \alpha[P_N(t+T) - P_N(t)]$, where $P_N(t+T) - P_N(t)$ is the power difference between successive symbols. The optimal scale factor for DPSK systems is precisely analogous to that for BPSK systems, and also approximately doubles the transmission distance.

In a practical system, phase-sensitive detection may yield the quadrature components, e.g., $\cos(\phi_R)$ and $\sin(\phi_R)$ in a PSK system [3][7]. Instead of correcting the phase by $\phi_R - \alpha P_N$, the corrected quadrature components can be calculated, e.g., as $\cos(\phi_R - \alpha P_N) = \sin(\phi_R)\sin(\alpha P_N) + \cos(\phi_R)\cos(\alpha P_N)$ and $\sin(\phi_R - \alpha P_N) = \sin(\phi_R)\cos(\alpha P_N) - \cos(\phi_R)\sin(\alpha P_N)$, using electronic signal processing techniques.

Other types of nonlinear phenomena may also limit the transmission distance in WDM systems. The interaction of the Kerr effect and optical amplifier noise also induces intensity noise [9], which we have ignored in this letter. Like [1], [5]-[6], this letter also ignores all dispersion and filtering effects.

IV. CONCLUSION

In systems using BPSK or DPSK, the impact of Kerr effect phase noise can be reduced by using electronic circuits to implement the Yin-Yang decision regions shown in Figs. 1. Equivalently, the received phase can be compensated as described above, in which case the receiver should employ the half-plane decision regions shown in Figs. 2. This compensation halves the STD of the residual nonlinear phase shift, permitting a doubling of the number of fiber spans and the transmission distance, assuming that Kerr effect phase noise is the dominant system impairment.

APPENDIX

A brief derivation of (2) to (4) is given here. Let m_x and σ_x^2 denote the mean and variance, respectively, of a random variable x . In this Appendix, for simplicity, the constant factor γL_{eff} is ignored. For a real value of $A = |E_0|$ and two complex circular Gaussian random variables ξ_1 and ξ_2 , from [10],

$$m_{|A+\xi_1|^2} = A^2 + 2\sigma_1^2,$$

$$\sigma_{|A+\xi_1|^2}^2 = f(\sigma_1^2) = 4A^2\sigma_1^2 + 4\sigma_1^4,$$

where $m_{|\xi_1|^2} = 2\sigma_1^2$ and the correlation is

$$E\left(|A+\xi_1|^2 - m_{|A+\xi_1|^2}\right)\left(|A+\xi_1 + \xi_2|^2 - m_{|A+\xi_1 + \xi_2|^2}\right) = f(\sigma_1^2).$$

Using the above expressions, the variance of (4) is

$$\sigma_{\phi_{NL}}^2(N) = \sum_{k=1}^N f(k\sigma^2) + 2 \sum_{k=1}^N (N-k) f(k\sigma^2),$$

where the first and second summations are for the square and correlation terms, respectively. The variance of (3) is

$$\begin{aligned} \sigma_{\phi_{NL} + \alpha P_N}^2(\alpha) = & \sigma_{\phi_{NL}}^2(N-1) + (\alpha-1)^2 f(N\sigma^2) - \\ & - 2(\alpha-1) \sum_{k=1}^{N-1} f(k\sigma^2). \end{aligned}$$

The optimal scale factor of (2) can be found by solving $d\sigma_{\phi_{NL} + \alpha P_N}^2(\alpha) / d\alpha = 0$ to obtain

$$\alpha = 1 + \frac{\sum_{k=1}^{N-1} f(k\sigma^2)}{f(N\sigma^2)}.$$

REFERENCES

- [1] J. P. Gordon and L. F. Mollenauer, "Phase noise in photonic communications systems using linear amplifiers," *Optics Letters*, vol. 15, pp. 1351-1353, Dec. 1990.
- [2] A. H. Gnauck *et al.*, "2.5 Tb/s (64 x 42.7 Gb/s) transmission over 40 x 100 km NZDSF using RZ-DPSK format and all-Raman-amplified spans," in *Proc. OFC '02*, postdeadline paper FC2.
- [3] R. A. Griffin *et al.*, "10 Gb/s optical differential quadrature phase shift key (DQPSK) transmission using GaAs/AlGaAs integration," in *Proc. OFC '02*, postdeadline paper FD6.
- [4] B. Zhu *et al.*, "Transmission of 3.2 Tb/s (80 x 42.7 Gb/s) over 5200 km of UltraWave™ fiber with 100-km dispersion-managed spans using RZ-DPSK format," in *Proc. ECOC '03*, postdeadline paper PD4.2.
- [5] X. Liu, X. Wei, R. E. Slusher, and C. J. McKinstrie, "Improving transmission performance in differential phase-shift-keyed systems by use of lumped nonlinear phase-shift compensation," *Optics Letters*, vol. 27, pp. 1616-1618, 2002.
- [6] C. Xu and X. Liu, "Postnonlinearity compensation with data-driven phase modulators in phase-shift keying transmission," *Optics Letters*, vol. 27, pp. 1619-1621, 2002.
- [7] S. Norimatsu, K. Iwashita, and K. Noguchi, "An 8 Gb/s QPSK optical homodyne detection experiment using external-cavity laser diodes," *IEEE Photon. Technol. Lett.*, vol. 4, pp. 765-767, 1992.
- [8] C. J. McKinstrie and C. Xie, "Phase jitter in single-channel soliton system with constant dispersion," *IEEE J. Sel. Top. Quantum Electron.*, vol. 8, pp. 616-625, 2002.
- [9] R. Hui, M. O'Sullivan, A. Robinson, and M. Taylor, "Modulation instability and its impact in multispan optical amplified IMDD systems: theory and experiments," *J. Lightwave Technol.*, vol. 15, pp. 1071-1082, July 1997.
- [10] J. G. Proakis, *Digital Communications*, 4th ed., Boston: McGraw Hill, 2000, p. 44.